Energy Proceedings
Vol 45, 2024
ISSN 2004-2965

3D Reconstruction and Quantitative Characterization of a NCM523 Cathode for Microstructure-Based Modeling

Jixiang Cai[1,3], Xuezhe Wei[1,3], Jiangong Zhu[1,3**], Bo Jiang[1,3], Xueyuan Wang[2,3], Jinding Liang[4], Haifeng Dai[1,3*]

1 School of Automotive Studies, Tongji University, 4800 Caoan Road, Shanghai, 201804, China

2 Department of Control Science and Engineering, Tongji University, 4800 Caoan Road, Shanghai, 201804, China

3 Clean Energy Automotive Engineering Center, Tongji University, 4800 Caoan Road, Shanghai, 201804, China

4 Contemporary Amperex Technology Co. Limited, Ningde, 352100, China
(*Corresponding Author: tongjidai@tongji.edu.cn)
(**Corresponding Author: zhujiangong@tongji.edu.cn)

ABSTRACT

Most mechanism-based battery models rely on the pseudo-two-dimensional (P2D) model, which simplifies electrode particles as homogenously distributed spheres, lacking the capability to represent the intricate microstructure. To develop a modeling approach aligned with authentic electrode microstructure, a mesoscopic image dataset of a NCM523 cathode is obtained through FIB-SEM, and, subsequently, the 3D microstructure model is reconstructed. Within this volume, we utilize thresholding methods to segment the active material (AM), the carbon-binder domain (CBD), and the pores. Furthermore, critical microstructural parameters, i.e., volume fractions, layer-by-layer area fractions of the three phases, equivalent diameter and sphericity distributions of AM particles, are quantified, Additionally, the pores phase undergoes connectivity analysis, and the tortuosity is also calculated. The results show significant heterogeneity in the electrode microstructure. In particular, only 33% of the particles can be regarded as spheres. This work demonstrates the limitations of the P2D model and can be used as the basis for microstructure-based battery modeling.

Keywords: lithium-ion battery, electrode microstructure, heterogeneity distribution, microstructural parameters, microstructure-based battery modeling

NONMENCLATURE

Abbreviations	
LIB	Lithium-ion battery
EV	Electric vehicle
P2D	Pseudo-two-dimensional
SAM	Simulated annealing method
NCM523	$LiNi_{0.5}Co_{0.2}Mn_{0.3}O_2$
FIB-SEM	Focused Ion Beam Scanning Electron Microscopy
AM	Active material
CBD	Carbon-binder domain

1. INTRODUCTION

The electrification of transportation has been rapidly advancing in recent years. Lithium-ion batteries (LIBs), serving as the primary power source for electric vehicles (EVs), have undergone significant development [1], resulting in a substantial increase in their energy density [2]. Nevertheless, to fully replace the traditional fuel-powered vehicles on a large scale, there remains a need to ensure high safety [3], long cycle life [4], and fast charging ability [5] of the LIBs.

The anode and cathode, as pivotal components of a battery, wield a profound influence on battery performance through their structural design. In battery manufacturing factories, the prevailing method for electrode development has traditionally been trial and error. This approach involves producing electrodes with diverse structures and subjecting them to a battery performance assessment using a series of electrochemical test methods. Then, manufacturers can establish a correlation between electrode structure and battery performance, enabling them to tailor battery designs to specific requirements. However, this approach entails substantial financial and time

This is a paper for 15th International Conference on Applied Energy (ICAE2023), Dec. 3-7, 2023, Doha, Qatar.

investments. Thus, some studies have ventured into electrode structure optimization through simulation methods as an alternative [6, 7].

The most commonly used simulation model is the pseudo-two-dimensional (P2D) electrochemical model proposed by Doyle and Newman [8]. This model is grounded in the porous electrode theory and concentrated solution theory. It entails solving a series of partial differential equations to obtain the internal and external characteristics of the battery, including the distribution of lithium-ion concentration and the terminal voltage. Many researchers have optimized the electrode structure, such as porosity [9], thickness [10], and aspect ratio [11], using this model. These optimizations have led to a significant improvement in the energy density and power density of the battery. Appiah et al. [12] adopted a mathematical model, which simulated multiple types of particles with different contact resistances in a single electrode, to study the effects of the different cathode thicknesses and porosities on lithium-ion transport. The relation between cathode designs and electrochemical performance was exhibited and the cathode designs were optimized for higher specific energy/power using a Ragone plot. Apart from the energy/power density, large-format LIBs also have a focused problem with product life due to temperature deviation. Lee et al. [13] established a 3D electrochemical-thermal coupled model of a 55 Ah large-format LIBs to analyze the effect of cell aspect ratios on thermal behavior during discharge. Results showed that when the cell aspect ratio became far from 2.15, heat generation turned non-uniform and the temperature deviation increased. However, it is important to note that the P2D model assumes that the electrode particles are uniformly distributed spheres. As a result, these models lack the capability to represent the intricate microstructure of the electrode at the particle scale, which is essential for guiding the design process.

In fact, the microstructure of the electrode plays a significant role in battery performance, especially lifespan and safety. In LIBs, lithium ions are inserted into or extracted from the active particles. This process induces volumetric deformation and generates localized stress concentrations due to the heterogeneous microstructure of the particles, contributing to localized particle cracking within the electrode [14]. In addition, the heterogeneous particle and pore size distributions lead to locally high current densities, resulting in a non-uniform state of lithiation [15] and hot spot formation [16]. Lithium dendrites may grow rapidly at these hot spots [17], ultimately leading to serious battery degradation and safety issues. Hence, it is essential to conduct an analysis of the electrode microstructure, establish the battery model at the mesoscopic scale, and reveal the interplay between the electrode microstructure and battery performance.

The first step in microstructure-based modeling involves the 3D reconstruction of electrodes. Several numerical methods have been used to reconstruct random electrode structures, including the Gauss stochastic field method [18], simulated annealing method (SAM) [19], process-based reconstruction [20], and stochastic grid method [21], etc. The SAM is regarded as providing the most realistic representation of electrode microstructures. He et al. [22] developed an ellipsoid-based simulated annealing method and numerically reconstructed the 3D microstructure of a graphite anode. However, while this method is known for its simplicity and convenience, the randomly reconstructed structures often rely on standard shapes such as spheres and ellipsoids. This simplification and smoothing of electrode particle morphology cannot accurately capture the true microstructure features, resulting in significant limitations. Thus, it is essential to obtain electrode microstructures through an image-based method.

In this paper, a mesoscopic image dataset of a $LiNi_{0.5}Co_{0.2}Mn_{0.3}O_2$ (NCM523) cathode is obtained through Focused Ion Beam Scanning Electron Microscopy (FIB-SEM). Subsequently, it is processed and reconstructed into a true 3D structure. In addition, critical structural parameters of the electrode are quantified, and the heterogeneity of the electrode is unveiled.

2. METHODOLOGIES

2.1 Sample preparation and FIB-SEM test

The electrode sample used in this work is extracted from a commercial pouch battery with a capacity of 1 Ah. The dry battery experiences an initial activation process involving electrolyte injection and chemical formation steps. Subsequently, the battery is disassembled inside a glove box, and the positive electrode is carefully cropped. It is then stored in a vacuum environment to prevent oxidation from the air.

The image dataset of the NCM523 is obtained through FIB-SEM, and its working principle is illustrated in Fig. 1. Thin layers of material are removed by ion column milling from the exposed surface towards the inner part, followed by electron column imaging of each newly exposed surface. As a result, a series of

consecutive SEM images with good contrast are obtained, providing input for 3D reconstruction. The pixel size of the SEM images is 63.4 nm, and the slice thickness is set to be 50 nm. In this work, the x-axis is associated with the thickness direction of electrode, and the direction along the x-axis points from the separator to the current collector.

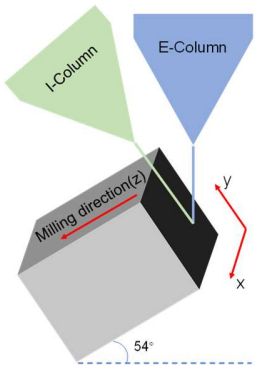

Fig. 1. Working principle of FIB-SEM

2.2 *Image processing and 3D reconstruction*

Due to limitations inherent to the FIB-SEM instrument, clear imaging can be only achieved on the electron column imaging plane (x-y plane), shifted images are observed on both other planes (x-z and y-z plane). To facilitate subsequent quantitative analysis, the x-axis and z-axis are interchanged, and the z-axis represents the direction of electrode thickness, pointing from the separator to the current collector. As shown in Fig. $2a - 2c$, this adjustment allows for clear imaging on the y-z plane, while the displacement issue persists on the x-y and x-z plane.

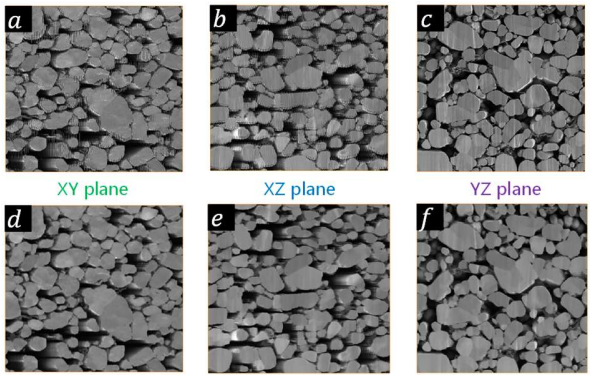

Fig. 2. Images before and after median filter
a – c before median filter; d – f after median filter

Filter methods are often used to process image data to improve image quality. Here, we employ median filter to smooth the images on all three planes, eliminating image noise and displacement issues. The images after the median filter are shown as Fig. $2d - 2f$, where the image quality in all three planes is almost consistent, with all of them exhibiting high sharpness.

The electrode comprises three distinct phases: the active material (AM), the carbon-binder domain (CBD), and the pores. To investigate the structure of each phase individually, the interactive thresholding segmentation method is employed based on the gray value. As illustrated in Fig. $3a - 3c$, the gray value ranges for the AM, CBD, and pores are set to 30152 – 58596, 23588 – 30151, and 7393 – 23587, respectively. Then, the 3D structures of the three separated phases are reconstructed using volume rendering, the results are presented as Fig. $3d - 3f$. Furthermore, these segregated phases can also be seamlessly integrated and depicted using three distinct colors, as illustrated in Fig. $3g$.

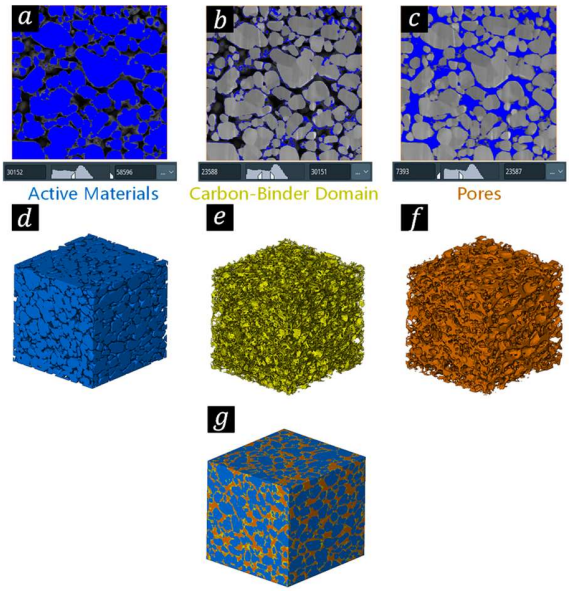

Fig. 3. Segmentation and 3D reconstruction process of three phases
a – c interactive thresholding; d – g 3D structures

2.3 *Quantitative characterization of key structures*

The volume fractions of the AM, CBD, and pores are fundamental geometrical characteristics of the electrode, which are crucial for understanding and modeling the behavior of electrode. Thus, they need to be calculated accurately from the reconstructed 3D structure to provide insights into the composition and distribution of these phases within the electrode.

The size and morphology of the AM, i.e., the particles, play a significant role in influencing the kinetics reaction at the solid-liquid interface and the lithium diffusion process within the particles. Additionally, the connectivity and tortuosity of the pores impact the transport of lithium ions within the electrolyte. Thus, it is imperative to conduct a quantitative analysis of these two phases separately.

3. RESULTS AND DISCUSSION

In this study, the volume fractions and layer-by-layer area fractions of three phases along the electrode thickness direction are obtained, the distributions of equivalent diameter and sphericity of the particles are expressed, the connectivity of pores is analyzed, and the tortuosity of each connecting segment is calculated using skeleton model. These analyses facilitate comparisons with the P2D model, providing valuable insights into the differences between the real microstructures and the simplified model.

3.1 Volume fraction and layer-by-layer area fractions

The volume fraction of the AM, CBD, and pores are presented in Table. 1. It is evident that AM, being the primary electrode component, constitutes nearly 70% of the total volume. Pores, serving as the pathways for lithium-ion transport, also account for a substantial portion, at approximately 23%. In contrast, CBD, functioning as an additive, comprises only around 8% of the total volume.

Table. 1. Volume fractions of three phases

Phase	AM	CBD	Pores
Volume Fraction	0.689276	0.0839781	0.226745

Fig. 4 illustrates the layer-by-layer area fractions of the three phases along the electrode thickness direction, where an increase in the slice number represents a gradual movement of the slice position from the separator to the current collector. From Fig. 4, the non-uniform distribution of the three phases in the electrode thickness direction can be seen. From the separator to the current collector, the area fractions of three phases fluctuate up and down near their volume fraction. It is noteworthy that the area fraction of AM significantly exceeds its volume fraction near the separator, while the area fraction of pores is notably lower than its volume fraction. This observation suggests that AM predominates in the region near the separator.

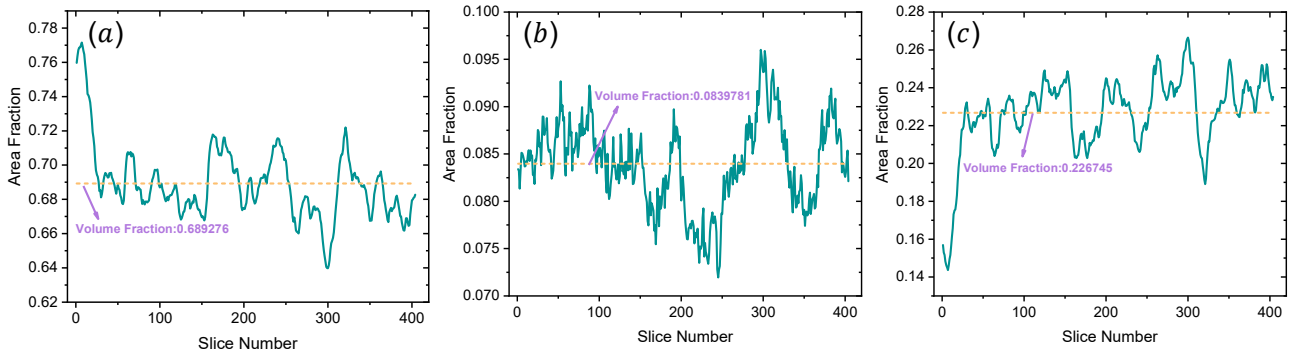

Fig. 4. Layer-by-layer area fraction of three phases
(a) AM; (b) CBD; (c) pores

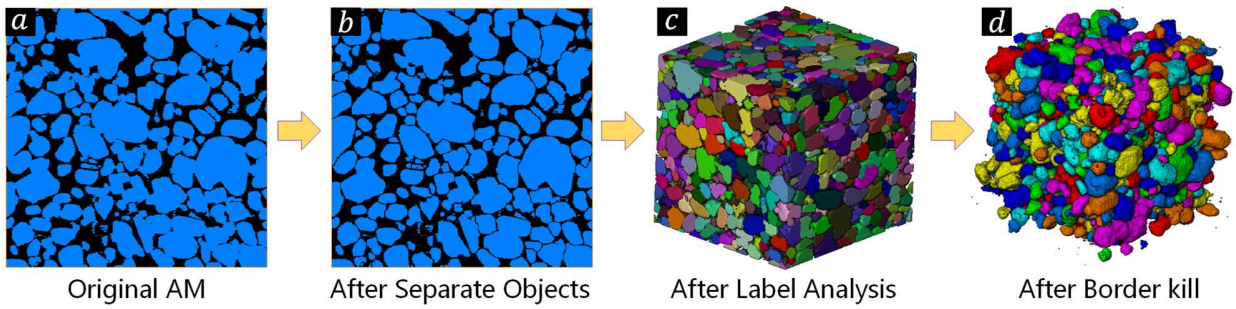

Fig. 5. Workflow for particle analysis

3.2 Equivalent diameters and sphericity of AM

The workflow for particle analysis is shown in Fig. 5. It can be seen from Fig. 5a that, errors in interactive thresholding segmentation lead to the unintended connection of several particles segmented based on gray values. Unexpectedly, these small particles are easily misconstrued as a single, larger particle in following analyses. To rectify this error, the initial images are processed using separate objects. As depicted in Fig. 5b, the particles initially assumed to be connected have been distinctly separated. Then, the shape of each particle is analyzed using the label analysis, as shown in Fig. 5c. From Fig. 5c, the presence of incomplete particles at the cube's edges can be observed, which can distort quantification results and are not the objects under study. To address this issue, the border kill is applied to

eliminate these edge particles, yielding the result presented in Fig. 5d.

Through an analysis of the size and morphology of each particle presented in Fig. 5 d , the equivalent diameter and sphericity of each particle can be obtained, as illustrated in Fig. 6. In Fig. 6(a), the distribution of the equivalent diameters of the particles along the thickness direction can be observed. The smaller particle numbers correspond to the positions near the separator, the opposite are near the current collector. The distribution of particle sizes appears approximately uniform in the direction of electrode thickness. However, within each cross-section, there is significant heterogeneity in particle sizes. The equivalent diameter of the largest particle can reach up to 6 μm, while the equivalent diameter of the smallest particle is even less than 1 μm.

Fig. 6(b) shows the distribution of sphericity of these particles. Sphericity values closer to 1 indicate that a particle tends to be a perfect sphere. In this analysis, the criteria is relaxed, considering sphericity values between 0.9 and 1.1 as indicative of a standard sphere. However, as shown in Fig. 6(b), only 33% of the particles meet this relaxed criterion. This further highlights the inappropriateness of assuming all particles as spheres in the P2D model.

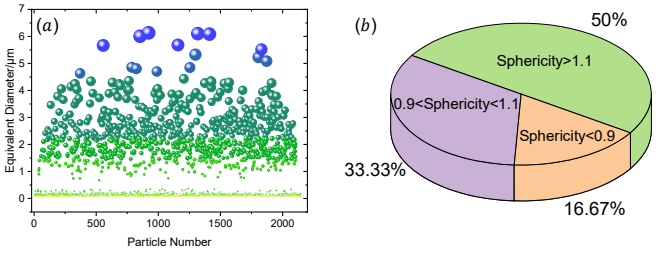

Fig. 6. Distribution of equivalent diameter and sphericity of particles
(a) equivalent diameter; (b) sphericity

3.3 Connectivity and tortuosity of pores

Pores are categorized into two groups: connected pores and isolated pores. Only connected pores allow the electrolyte to flow for charge transfer and ion diffusion. Thus, the connectivity of pores is essential. Following the connectivity analysis, the connected pores and the isolated pores are distinguished from the whole pores, as shown in Fig. 7a – 7c. It is shown that there are only several small isolated pores within the electrode, which has negligible impact on battery performance and may have originated from errors introduced during the interactive thresholding segmentation process.

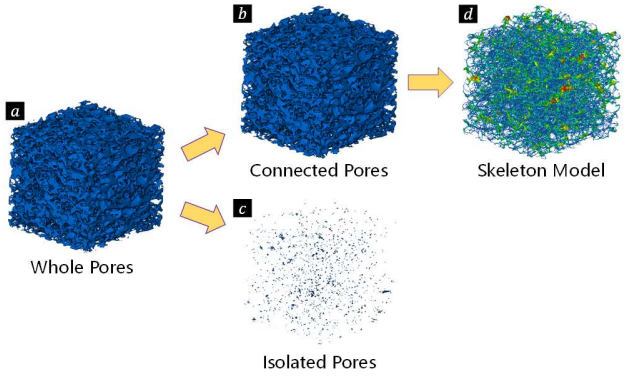

Fig. 7. Connectivity analysis and the skeleton model of pores

Tortuosity serves as a critical parameter in characterizing pore morphology within porous media, defined as the ratio of the actual length of the seepage channel to its linear length. A higher tortuosity implies reduced electrode permeability, longer lithium ion transport paths, and a negative impact on battery rate performance. The tortuosity of each segmented channel can be determined by transforming the connected pores into a skeleton model, as shown in Fig. 7d.

The calculated result of tortuosity is shown in Fig. 8. From Fig. 8, it's evident that the tortuosity of the majority of segmented channels falls within the range of 1 - 1.1. This reflects that the electrolyte can move easily within the connected pore space, resulting in excellent battery rate performance. Additionally, similar to the distribution of particle sizes and shapes, the distribution of pore tortuosity within the electrode is heterogeneous. This observation also emphasizes the need for adjustments to the P2D model to better capture the complexity of the real electrode.

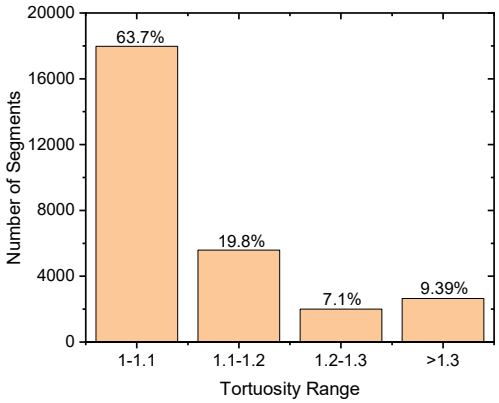

Fig. 8. Tortuosity distribution of the segments

4. CONCLUSIONS

Electrochemical modeling of LIBs plays a crucial role in optimizing electrode design to enhance battery safety, extend cycle life, and achieve faster charging. Presently, electrochemical models rely on the P2D model which assumes electrode particles to be uniformly distributed

spheres. This simplification overlooks the impact of the heterogeneity in the electrode microstructure on battery performance. Thus, it is imperative to accurately capture the real microstructure of electrodes and develop microstructure-based battery modeling methods that elucidate the correlation between electrode microstructure and battery performance. This insight may serve as a valuable directive for the effective refinement of electrode design.

The precise acquisition of electrode structure and quantification of its geometric features are the initial and pivotal steps in microstructure-based modeling. In this work, the mesoscopic image dataset of a NCM523 cathode is obtained using FIB-SEM, and is further processed and reconstructed into a 3D model. Subsequently, the particle size and sphericity distributions are analyzed, and the connectivity of pores is examined. Additionally, the tortuosity of each segmented channel is calculated. The results reveal the considerable heterogeneity of the electrode internal microstructure. This work holds significant value in exposing the limitations of the P2D model and will contribute to subsequent microstructure-based modeling endeavors.

ACKNOWLEDGEMENT

This research was funded by the Fundamental Research Funds for the Central Universities and the Major State Basic Research Development Program of China (973 Program, Grant No. 2022YFB2502302, Grant No. 2022YFB2502304).

DECLARATION OF INTEREST STATEMENT

The authors declare that they have no known competing financial interests or personal relationships that could have appeared to influence the work reported in this paper. All authors read and approved the final manuscript.

REFERENCE

[1] CAI J,ZHANG L,WANG X, et al.Investigation of an M-Sequence based impedance spectrum acquisition method for lithium-ion batteries from the engineering application perspective[J].Journal of Energy Storage,2023,59:

[2] XU J,CAI X,CAI S, et al.High‐Energy Lithium‐Ion Batteries: Recent Progress and a Promising Future in Applications[J].Energy & Environmental Materials,2023,6:

[3] QIU Y,JIANG F.A review on passive and active strategies of enhancing the safety of lithium-ion batteries[J].International Journal of Heat and Mass Transfer,2022,184:

[4] XIAO B,WU G,WANG T, et al.High-entropy oxides as advanced anode materials for long-life lithium-ion Batteries[J].Nano Energy,2022,95:

[5] WANG C Y,LIU T,YANG X G, et al.Fast charging of energy-dense lithium-ion batteries[J].Nature,2022,611:485-90.

[6] CAMPBELL I D,GOPALAKRISHNAN K,MARINESCU M, et al.Optimising lithium-ion cell design for plug-in hybrid and battery electric vehicles[J].Journal of Energy Storage,2019,22:228-38.

[7] COUTO L D,CHARKHGARD M,KARAMAN B, et al.Lithium-ion battery design optimization based on a dimensionless reduced-order electrochemical model[J].Energy,2023,263:

[8] DOYLE M,FULLER T F,NEWMAN J.Modeling of galvanostatic charge and discharge of the lithium/polymer/insertion cell[J].J Electrochem Soc,1993,140:1526.

[9] DAI Y,SRINIVASAN V.On Graded Electrode Porosity as a Design Tool for Improving the Energy Density of Batteries[J].J Electrochem Soc,2015,163:A406-A16.

[10] XU M,REICHMAN B,WANG X.Modeling the effect of electrode thickness on the performance of lithium-ion batteries with experimental validation[J].Energy,2019,186:

[11] LEE J-J,KIM J-S,LEE D-C, et al.Design optimization of tab attachment positions and cell aspect ratio to minimize temperature difference in 45-Ah LFP large-format lithium-ion pouch cells[J].Applied Thermal Engineering,2021,182:

[12] APPIAH W A,PARK J,SONG S, et al.Design optimization of LiNi0.6Co0.2Mn0.2O2/graphite lithium-ion cells based on simulation and experimental data[J].Journal of Power Sources,2016,319:147-58.

[13] LEE D-C,LEE J-J,KIM J-S, et al.Thermal behaviors analysis of 55 Ah large-format lithium-ion pouch cells with different cell aspect ratios, tab locations, and C-rates[J].Applied Thermal Engineering,2020,175:

[14] CLERICI D,MOCERA F,SOMà A.Analytical Solution for Coupled Diffusion Induced Stress Model for Lithium-Ion Battery[J].Energies,2020,13:

[15] XU Y,HU E,ZHANG K, et al.In situ Visualization of State-of-Charge Heterogeneity within a LiCoO2 Particle that Evolves upon Cycling at Different Rates[J].ACS Energy Letters,2017,2:1240-5.

[16] FOROUZAN M M,MAZZEO B A,WHEELER D R.Modeling the Effects of Electrode Microstructural Heterogeneities on Li-Ion Battery Performance and Lifetime[J].J Electrochem Soc,2018,165:A2127-A44.

[17] HAMEDI A-S,POURAGHAJAN F,SUN F, et al.Interplay of Electrode Heterogeneity and Lithium Plating[J].J Electrochem Soc,2022,169:
[18] FEINAUER J,BRERETON T,SPETTL A, et al.Stochastic 3D modeling of the microstructure of lithium-ion battery anodes via Gaussian random fields on the sphere[J].Computational Materials Science,2015,109:137-46.
[19] WU W,JIANG F.Simulated annealing reconstruction and characterization of the three-dimensional microstructure of a LiCoO2 lithium-ion battery cathode[J].Materials characterization,2013,80:62-8.
[20] SIDDIQUE N,LIU F.Process based reconstruction and simulation of a three-dimensional fuel cell catalyst layer[J].Electrochimica Acta,2010,55:5357-66.
[21] STEPHENSON D E,HARTMAN E M,HARB J N, et al.Modeling of particle-particle interactions in porous cathodes for lithium-ion batteries[J].J Electrochem Soc,2007,154:A1146.
[22] HE S,ZENG J,HABTE B T, et al.Numerical reconstruction of microstructure of graphite anode of lithium-ion battery[J].Science Bulletin,2016,61:656-64.